SUPPLEMENTAL TEXT

ETI triggers repression of *SUC2* gene, which provides an explanation for why the *SUC2* endogene and the *amiR-SUL* transgene were found repressed in *$35S_{pro}$:HopT1-1/$SUC2_{pro}$:amiRSUL* plants exhibiting dwarf statures.

When we molecularly characterized independent T2 transgenic lines expressing *$35S_{pro}$:HopT1-1* in the *$SUC2_{pro}$:amiR-SUL* background, we noticed that the basal expression of the *SUC2* gene and of the *amiR-SUL* transgene was significantly decreased in plants exhibiting strong developmental defects such as the *$35S_{pro}$:HopT1-1*#7 and #11 transgenic lines shown in Figure 3A (Figure S6D and S6E). Importantly, the dwarf stature of these transgenic plants was associated with a strong constitutive *PR1* expression (Figure S6B), suggesting that the repression of the *SUC2* endogene and of the *amiR-SUL* transgene could be caused by the high ETI response detected in these backgrounds. To test this possibility, we repeated these molecular analyses in transgenic lines exhibiting lower accumulation of HopT1-1 mRNAs such as the *$35S_{pro}$:HopT1-1*#17 reference line (Figure S6B). As expected, this line displayed lower constitutive expression of *PR1* and milder developmental defects than the ones observed in lines #7 and #11 (Figure S6A and S6C), indicating that the ETI response is attenuated in this background. Furthermore, we observed a significantly lower repression of both the *SUC2* endogene and the *amiR-SUL* transgene in the *$35S_{pro}$:HopT1-1*#17 line compared with lines #7 and #11 (Figure S6D and S6E), suggesting that the repression of *SUC2* and of the *amiR-SUL* transgene is indeed directly linked with the level of ETI activation. This result is also consistent with unaltered changes in SUL siRNA levels observed in *$35S_{pro}$:HopT1-1*/*$SUC2_{pro}$:IR-SUL* (*Suc-Sul*) transgenic plants exhibiting intermediate developmental phenotypes as compared to *Suc-Sul* parental plants (Navarro et al., 2008). To

confirm the above conclusion, we have additionally monitored the basal expression of the *SUC2* endogene in Arabidopsis transgenic plants that conditionally express the bacterial effector AvrRpm1 (*DEX_{pro}:AvrRpm1)*, which is known to trigger a strong ETI response in the Arabidopsis Col-0 accession due to RPM1-dependent recognition of this effector (Debener et al., 1991; Grant et al., 1995). Upon dexamethasone application we also detected a down-regulation of *SUC2* transcript level that was anti-correlated with the level of *PR1* mRNAs, supporting a role for ETI in repressing the basal expression of *SUC2*. Altogether, these data indicate that the decrease in *SUC2* and in *amiR-SUL* transgene mRNA levels observed in the dwarf *$35S_{pro}$:HopT1-1*#7 and #11 plants is likely due to the strong ETI response triggered in those specific plants.

REFERENCES

Debener, T., Lehnackers, H., Arnold, M., Dangl, J.L. (1991). Identification and molecular mapping of a single Arabidopsis thaliana locus determining resistance to a phytopathogenic Pseudomonas syringae isolate. Plant Journal *1*, 289-302.

Grant, M.R., Godiard, L., Straube, E., Ashfield, T., Lewald, J., Sattler, A., Innes, R.W., Dangl, J.L. (1995). Structure of the Arabidopsis *RPM1* gene enabling dual specificity disease resistance. Science *269*, 843-846.

SUPPLEMENTAL FIGURE LEGENDS

Supplemental Figure 1. The growth defect of the *Pto* Δ*hopT1-1* strain is specifically rescued in Arabidopsis miRNA-defective mutants.

Five-week-old Col-0 Arabidopsis (WT) plants and indicated genotypes in each panel were dip-inoculated with bacterial strain *Pto* DC3000 (*Pto*) (blue dots), *Pto* Δ*hopT1-1* (green dots) or *Pto* Δ*hopC1* (orange dots) at a concentration of 10^8 cfu/mL. At three days post-inoculation, leaves from three plants were collected and bacterial titers were monitored. Each dot represents number of bacteria as log (cfu per cm^2) and mean (n=8 or 16) is represented as horizontal line in the dot plots. Statistical significance was assessed using the ANOVA test (n.s.: p-value>0.05; *: p-value<0.01; **: p-value<0.001; ***: p-value<0.0001; ****: p-value<0.00001). Independent biological replicates distinct from one presented in Figure 1 are presented here. **(A)-(B)**: Three different *ago1* mutants, namely *ago1-25*, *ago1-26* and *ago1-27,* exhibit no significant difference (n.s.) in the growth of *Pto* Δ*hopT1-1* strain as compared to *Pto* DC3000 strain, rescuing growth defect of *Pto* Δ*hopT1-1* observed in WT plants. The growth of the *Pto* Δ*hopC1* remained significantly different as compared to the titer of *Pto* DC3000 in *ago1-27* mutant, similar to WT plants. **(C)** Other *ago* mutants, *ago2-1, ago4-2* and *ago4-3,* could not rescue the growth defect of *Pto* Δ*hopT1-1* when compared to *Pto* DC3000. **(D)-(E)** miRNA biogenesis mutants, *se-1* and *dcl1-11*, exhibited a rescue in the growth defect of *Pto* Δ*hopT1-1*, similar to *ago1* mutants. The growth defect of *Pto* Δ*hopC1* was not rescued in *se-1* when compared to WT plants. **(F)-(G)** The growth defect of the *Pto ΔhopT1-1* strain*,* when compared to the *Pto* DC3000, is not rescued in siRNA biogenesis mutants: *rdr1-1 rdr2-1 rdr6-15*, *dcl2-1 dcl4-2* and *sgs3-1*.

Supplemental Figure 2. HopT1-1 possesses conserved GW motifs and does not interfere with endogenous miRNA accumulation.

(A) Protein sequence alignment between the *Pseudomonas syringae* pv. *tomato* (*Pto* DC3000) HopT1-1 (NP_808678.1), HopT1-2 (NP_794344.1), HopT2 (NP_794341.1) and the *Marinomonas mediterranea* MMB-1 HopT1-1 (WP_013659626.1). These protein sequences possess three conserved GW motifs, highlighted in bold and marked with red asterisks. **(B)** Two independent T2 transgenic lines of *SUC2$_{pro}$:amiR-SUL* expressing HopT1-1 and HopT1-1m3 were selected, respectively. Relative mRNA level of *HopT1-1* transcript in these lines was monitored in comparison to WT1 and WT2, respectively by RT-qPCR analysis using *ACTIN2* as a control. Error bars represent the standard deviation from three technical replicates. **(C)** Accumulation level of endogenous mature miRNAs, miR156, miR160 and miR168 in plants described in (B) was evaluated by RT-qPCR analysis using adaptor-ligated primers. *ACTIN2* was used as a control. Error bars represent the standard deviation from three technical replicates. No significant difference was observed in miRNA accumulation in the presence of HopT1-1 or HopT1-1m3, indicating that HopT1-1 does not interfere with mature miRNA accumulation.

Supplemental Figure 3. Protein accumulation level of HopT1-1 and of HopT1-1m3 transiently expressed *N. benthamiana* leaves

(A) *Agrobacterium tumefaciens* strains carrying *Myc-HopT1-1* or *Myc-HopT1-1m3* constructs were infiltrated in four-week-old *N. benthamiana* leaves. Non-infiltrated *N. benthamiana* leaves were used as a control. Protein accumulation level of HopT1-1 and of HopT1-1m3 was monitored at 3 dpi by immunoblotting. Arrow indicates the

band corresponding specifically to HopT1-1 and HopT1-1m3 detected using anti-Myc antibody. Relative quantification was performed using the unspecific proteins (*) detected by anti-Myc antibody. Both the proteins exhibit stable accumulation *in planta*. **(B)** To perform FRET-FLIM analysis, four-week-old *N. benthamiana* leaves were infiltrated with CFP-AGO1 alone or with YFP-tagged HopT1-1 or HopT1-1m3. After 2 dpi, protein accumulation level was monitored by immunoblotting using anti-GFP antibody. Ponceau staining was used to show equal protein loading for each sample. **(C)** Same as (B), but using CFP-AGO1 alone or with HopT1-1-HA.

Supplemental Figure 4. Characterization of dexamethasone inducible HopT1-1 and HopT1-1m3 transgenic lines

(A) Five-week-old Arabidopsis Col-0 (WT) plants and T2 transgenic lines expressing Myc-HopT1-1 or Myc-HopT1-1m3 under the control of the dexamethasone inducible promoter (DEX_{pro}:*HopT1-1* and DEX_{pro}:*HopT1-1m3*, respectively) were sprayed using 30 µM of DEX. After 24 hours, leaves from three plants were collected and pooled together for the transgenic lines as well as for the control line for further analyses. Protein accumulation of HopT1-1 and of HopT1-1m3 was assessed by immunoblotting using anti-Myc antibody. Coomassie staining shows equal protein loading for each sample. Transgenic lines expressing comparable levels of HopT1-1 and of HopT1-1m3 were selected for further analyses. **(B)** The plants described in (A) were sprayed every 24 hours using Mock solution or 30 µM of DEX. Leaves were collected 48 hours post induction. Relative expression quantification of *HopT1-1* and of *HopT1-1m3* transcript level in Mock and DEX-treated plants was done using RT-qPCR analysis. Error bars represent the standard deviation from three technical replicates. Mock treated DEX_{pro}:*HopT1-1* and DEX_{pro}:*HopT1-1m3* lines did not show

leaky expression of the respective transcripts. **(C)** ROS production assay upon flg22 treatment was performed on the mock-treated plants described in (B). Each dot represents luminescence (RLU) captured for each technical replicate (n=24) and the mean is indicated by horizontal bar. In mock condition, the *HopT1-1* transgenic lines did not exhibit significant reduction in ROS production when compared to WT and HopT1-1m3 plants. Statistical significance was assessed using the ANOVA test (NS: p-value>0.05; ****: p-value<0.0001).

Supplemental Figure 5. Accumulation level of streptavidin-associated peptides containing each GW and GF motifs of HopT1-1 and HopT1-1m3, respectively (Supports Fig 2E)

To perform the pull-down experiment, we first assessed the accumulation level of streptavidin-associated peptides containing each GW and GF motifs of HopT1-1 and HopT1-1m3, respectively by using dot blot assay. The biotinylated peptides were immobilized with HRP-streptavidin beads then were spotted on to the nitrocellulose membrane at three different amounts (1 µg, 0.1 µg and 0.01 µg). The presence of peptides was revealed by adding ECL substrate.

Supplemental Figure 6. ETI response represses the expression of the *SUC2* gene and of the *SUC2*$_{pro}$:*amiR-SUL* transgene

(A) Representative pictures of five-week-old *SUC2*$_{pro}$*:amiR-SUL* plants (WT) along with *SUC2*$_{pro}$*:amiR-SUL* transgenic line overexpressing HopT1-1. The selected HopT1-1#17 transgenic line exhibit intermediate phenotype compared to the lines described in Figure 5. Transgenic lines described in here and in Figure 5 were subjected to further molecular analysis. **(B)** Relative *HopT1-1* mRNA level was

monitored in HopT1-1#17 line by RT-qPCR analysis and the first graph is recapitulated from Figure S2 to compare *HopT1-1* expression level between the different transgenic lines. *Ubiquitin* was used as a control and the error bars represent the standard deviation from three technical replicates. The *HopT1-1* transcript accumulation in the transgenic line exhibiting intermediate phenotype was approximately 10 times less compared to the lines described in Figure 5. **(C)** Same as in (B), but *PR1* mRNA level was monitored in HopT1-1#17 line and the first graph is recapitulated from Figure 5 to compare *PR1* expression level between the different transgenic lines. **(D)** Relative *SUC2* mRNA level was monitored by RT-qPCR analysis using the same samples as described in (B). *Ubiquitin* was used as a control and the error bars represent the standard deviation from three technical replicates. **(E)** Same as in (D) but, relative *amiR-SUL* transgene transcript level was monitored. **(F)-(G)** Five-week-old Col-0 Arabidopsis (WT) plants and DEX_{pro}*:AvrRpm1* transgenic plants were sprayed using 30 µM of DEX. Leaves were collected at 6 and 9 hours post-treatment to assess the relative mRNA levels of *PR1* and *SUC2* by using RT-qPCR analysis. *Ubiquitin* was used as a control and the error bars represent the standard deviation from three technical replicates.

Supplemental Figure 7. The accumulation of the pri-miRNAs, *pri-miR171c* and *pri-miR166a* is not affected in the HopT1-1 transgenic lines

The accumulation level of primary miRNA (pri-miRNA) transcripts of *pri-miR171c* and *pri-miR166a* in the transgenic plants expressing HopT1-1 or HopT1-1m3 compared with WT1 or WT2, respectively was assessed by semi-quantitative RT-PCR analysis. Arabidopsis mutant defective in miRNA biogenesis (*dcl1-9* in La-*er* background) was used as a control. *Ubiquitin10* was used as a loading control. No significant

difference was observed in the accumulation of these pri-miRNAs in the presence of HopT1-1 or HopT1-1m3, respectively.

Supplemental Figure 8. Constitutive expression of HopT1-1 induces a *PAD4/SID2*-dependent autoimmune phenotype in Arabidopsis

(A) Representative pictures of five-week-old Col-0 (WT) Arabidopsis plants along with three different classes of primary transgenic plants (T1) expressing Myc-HopT1-1. Leaves from plants showing similar phenotype were pooled and used for further molecular analyses. The accumulation level of Myc-HopT1-1 and of AGO1 proteins were assessed by immunoblotting using anti-Myc and anti-AGO1 antibodies. Coomassie staining shows equal protein loading for each sample. Transgenic plants belonging to class I exhibit detectable levels of Myc-HopT1-1 as well as overaccumulation of AGO1 protein when compared to WT plants and other classes, respectively. (**B**) Representative pictures of *pad4 sid2* plants and transgenic lines expressing HopT1-1 in *pad4 sid2*. (**C**) Relative mRNA accumulation level of *HopT1-1* and of *PR1* was performed by RT-qPCR analysis using the same set of data for HopT1-1 expressing $SUC2_{pro}$*:amiR-SUL* transgenic lines as described in Figure S6 and the plants expressing HopT1-1 in *pad4 sid2*. *ACTIN2* was used as control. Error bars represent the standard deviation from three technical replicates. The *pad4 sid2* double mutations partially compromise the HopT1-1-triggered developmental defects and the SA-dependent defense response. (**D**) Relative mRNA accumulation of CNL or TNL transcripts that are targeted by miRNAs and/or siRNAs was monitored by RT-qPCR analysis in $SUC2_{pro}$*:amiR-SUL* transgenic lines overexpressing HopT1-1. *ACTIN2* was used as control. Error bars represent the standard deviation from three technical replicates. No significant difference was observed in the expression of

these genes at the transcript level.

Supplemental Figure 9. Stable expression of an *AGO1* transgene that is refractory to miR168 action induces *PAD4/SID2*-dependent autoimmune phenotype in Arabidopsis

(A) Representative pictures of six-week-old Col-0 plants (WT) along with primary transgenic plants (T1) expressing *AGO1*$_{pro}$*:AGO1* (WT-*AGO1*; upper panel) and miR168 refractory *AGO1* transgene *AGO1*$_{pro}$*:4m-AGO1* (*4m-AGO1*; lower panel) under the native *AGO1* promoter in WT background. Primary transformants of *4m-AGO1* exhibit two different phenotypes, WT-like and mir-AGO1. mir-AGO1 plants show dwarf and anthocyaned phenotype whereas WT-like plants show normal phenotype similar to WT plants. **(B)** Relative *AGO1* mRNA level in WT plants and in *WT-AGO1* as well as in *4m-AGO1* transgenic plants exhibiting WT-like and mir-AGO1 phenotype was monitored by RT-qPCR analysis using *Ubiquitin* as control. Error bars represent the standard deviation from three technical replicates. The level of AGO1 protein was assessed by immunobloting in the same samples. Ponceau staining shows equal loading for each sample. **(C)** Relative mRNA accumulation level of SA responsive genes (*PR1* and *PR2*) in same samples as (B) was monitored by RT-qPCR analysis using *Ubiquitin* as control. **(D)** Six-week-old primary transgenic plants (T1 generation) expressing *4m-AGO1* transgene in WT and in different SA signalling mutants (*ndr1* and *pad4 sid2*) and SA biosynthesis mutant (*sid2*) exhibiting WT-like and miR-AGO1 phenotypes were collected. Relative mRNA accumulation level of *AGO1* and of SA responsive genes (*PR1*, *PR2* and *PR5*) or gene involved in salicylic acid biosynthesis (*ICS1*) was monitored using RT-qPCR analysis same as described in (B)-(C). **(E)** Relative mRNA accumulation level of cell death and

senescence-related markers (*ALD1* and *WRKY75*) in same samples as (D) was monitored by RT-qPCR analysis using *Ubiquitin* as control. **(F)** WT plants and primary transgenic plants expressing *4m-AGO1* transgene were grown in parallel at 23°C and at 28°C. Leaves from four-week-old plants were collected to assess the level of *AGO1* and *PR1* mRNA accumulation by RT-qPCR using *Ubiquitin* as a control.

Supplemental Figure 10. Several effectors encoded by agriculturally important phytopathogens contain canonical GW/WG motifs

Effectors encoded by bacteria (*Xanthomonas campestris*, *Xanthomonas oryzae* and *Xyllela fastidiosa*), oomycetes (*Phytophthora infestans* and *Phytophthora sojae*) or fungi (*Puccinia graminis* and *Fusarium graminearum*) containing the highest score (matrix AGO-planVir) of GW/WG motifs prediction were retrieved by using the web portal http://www.comgen.pl/whub (Zielezinski A. & Karlowski WM, 2014). A red bar represents each GW or WG motif.

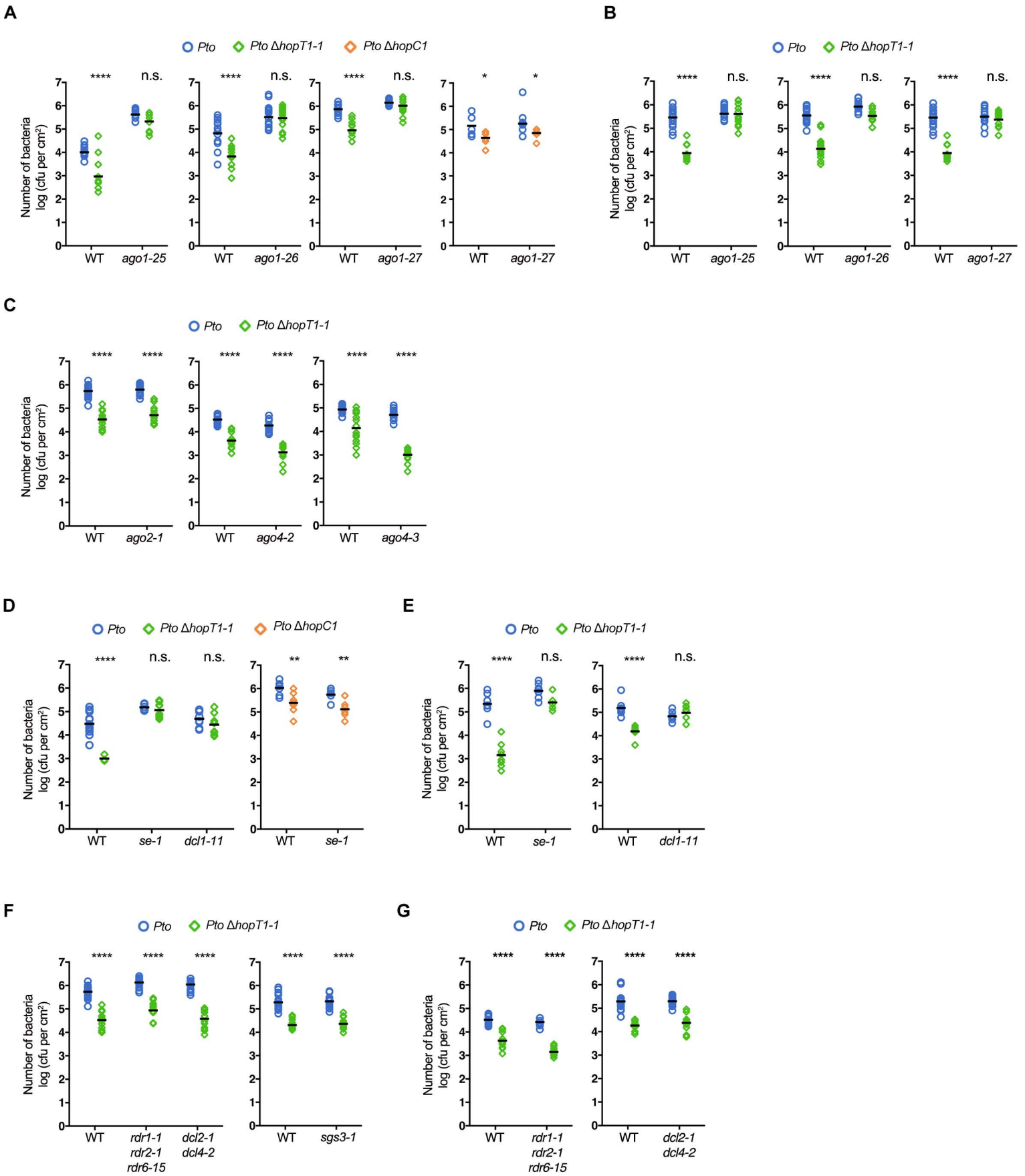

Supplemental Figure 1. The growth defect of the Pto ΔhopT1-1 strain is specifically rescued in Arabidopsis miRNA-defective mutants
Five-week-old Col-0 Arabidopsis (WT) plants and indicated genotypes in each panel were dip inoculated with bacterial strain *Pto* DC3000 (*Pto*) (blue dots), *Pto* Δ*hopT1-1* (green dots) or *Pto* Δ*hopC1* (orange dots) at a concentration of 10^8 cfu/mL. At three days post-inoculation, leaves from three plants were collected and bacterial titers were monitored. Each dot represents number of bacteria as log (cfu per cm^2) and mean (n=8 or 16) is represented as horizontal line in the dot plots. Statistical significance was assessed using the ANOVA test (n.s.: p-value>0.05; *: p-value<0.01; **: p-value<0.001; ***: p-value<0.0001; ****: p-value<0.00001). Independent biological replicates distinct from one presented in Figure 1 are presented here. **(A)-(B)** Three different ago1 mutants, namely *ago1-25*, *ago1-26* and *ago1-27*, exhibited no significant difference (n.s.) in the growth of *Pto* Δ*hopT1-1* strain as compared to *Pto* DC3000 strain, rescuing growth defect of *Pto* Δ*hopT1-1* observed in WT plants. The growth of the *Pto* Δ*hopC1* remained significantly different as compared to the titer of *Pto* DC3000 in *ago1-27* mutant, similar to WT plants. (C) Other *ago* mutants, *ago2-1*, *ago4-2* and *ago4-3*, could not rescue the growth defect of *Pto* Δ*hopT1-1* when compared to Pto DC3000. **(D)-(E)** miRNA biogenesis mutants, *se-1* and *dcl1-11*, exhibited a rescue in the growth defect of *Pto* Δ*hopT1-1*, similar to *ago1* mutants. The growth defect of *Pto* Δ*hopC1* was not rescued in *se-1* when compared to WT plants. **(F)-(G)** The growth defect of the *Pto* Δ*hopT1-1* strain, when compared to the *Pto* DC3000, is not rescued in siRNA biogenesis mutants: *rdr1-1 rdr2-1 rdr6-15*, *dcl2-1 dcl4-2* and *sgs3-1*.

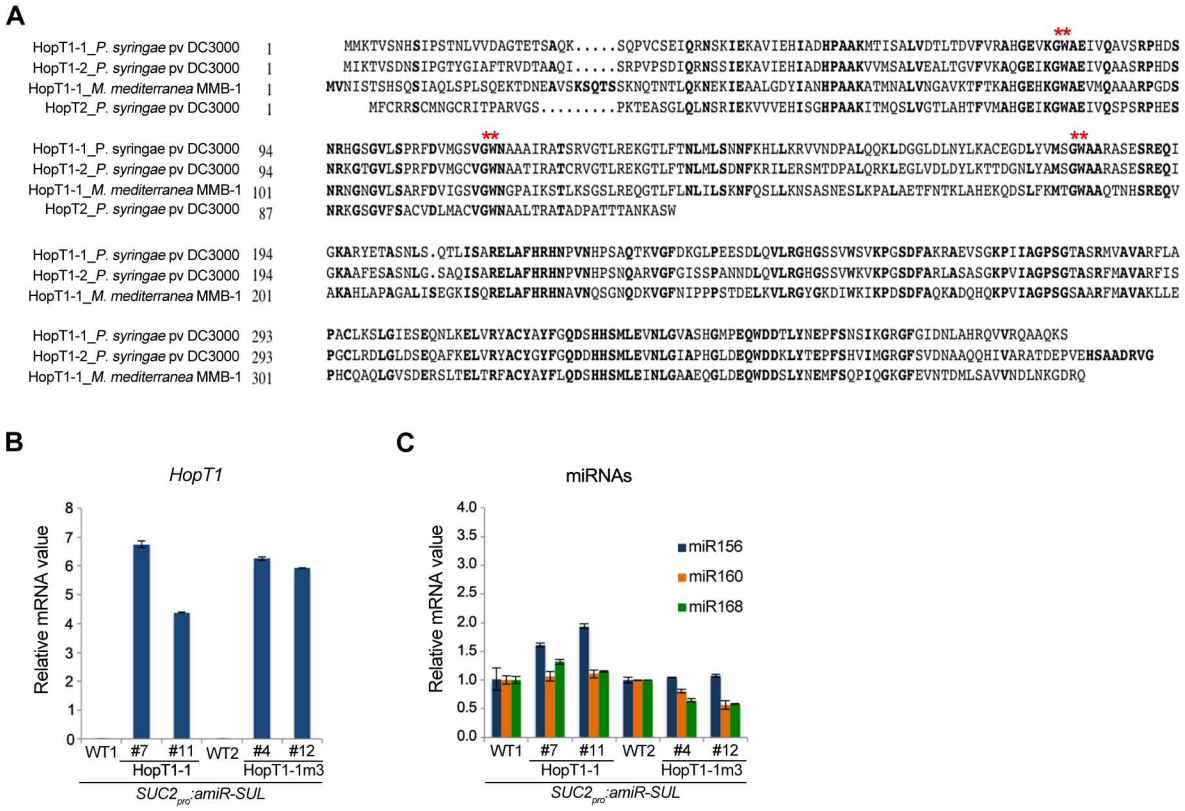

Supplemental Figure 2. HopT1-1 possesses conserved GW motifs and does not interfere with endogenous miRNA accumulation.
(A) Protein sequence alignment between the *Pseudomonas syringae* pv. tomato (*Pto* DC3000) HopT1-1 (NP_808678.1), HopT1-2 (NP_794344.1), HopT2 (NP_794341.1) and the *Marinomonas mediterranea* MMB-1 HopT1-1 (WP_013659626.1). These protein sequences possess three conserved GW motifs, highlighted in bold and marked with red asterisks. **(B)** Two independent T2 transgenic lines of *SUC2$_{pro}$:amiR-SUL* expressing HopT1-1 and HopT1-1m3 were selected, respectively. Relative mRNA level of *HopT1* transcript in these lines was monitored in comparison to WT1 and WT2, respectively by RT-qPCR analysis using *ACTIN2* as a control. Error bars represent the standard deviation from three technical replicates. **(C)** Accumulation level of endogenous mature miRNAs, miR156, miR160 and miR168 in plants described in (B) was evaluated by RT-qPCR analysis using adaptor-ligated primers. *ACTIN2* was used as a control. Error bars represent the standard deviation from three technical replicates. No significant difference was observed in miRNA accumulation in the presence of HopT1-1 or HopT1-1m3, indicating that HopT1-1 does not interfere with mature miRNA accumulation.

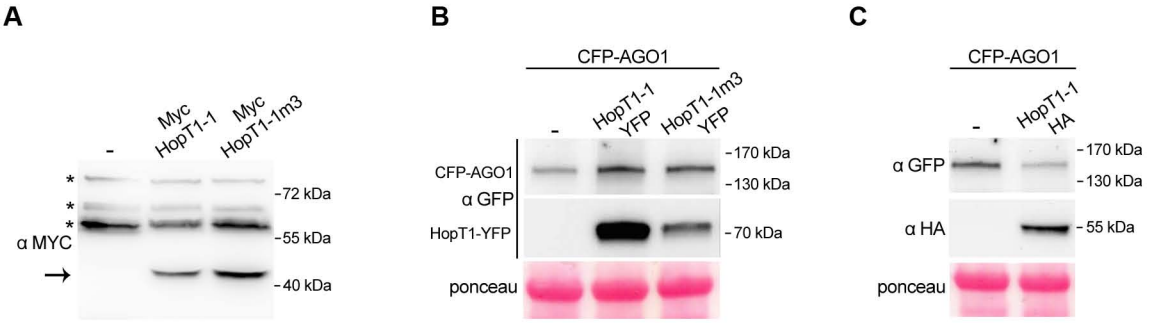

Supplemental Figure 3. Protein accumulation level of HopT1-1 and HopT1-1m3 transiently expressed in planta
(A) *Agrobacterium tumefaciens* strains carrying *Myc-HopT1-1* or *Myc-HopT1-1m3* constructs were infiltrated in four-week-old *N. benthamiana* leaves. Non-infiltrated *N. benthamiana* leaves were used as a control. Protein accumulation level of HopT1-1 and HopT1-1m3 was monitored at 3 dpi by immunoblotting. Arrow indicates the band corresponding specifically to HopT1-1 and HopT1-1m3 detected using anti-Myc antibody. Relative quantification was performed using the unspecific proteins (*) detected by anti-Myc antibody. Both the proteins exhibit stable accumulation *in planta*. **(B)** To perform FRET/FLIM analysis, four-week-old *N. benthamiana* leaves were infiltrated with CFP-AGO1 alone or with YFP-tagged HopT1-1 or HopT1-1m3. After 2 dpi, protein accumulation level was monitored by immunoblotting using anti-GFP antibody. Ponceau staining was used to show equal protein loading for each sample. **(C)** Same as (B), but using CFP-AGO1 alone or with HopT1-1-HA.

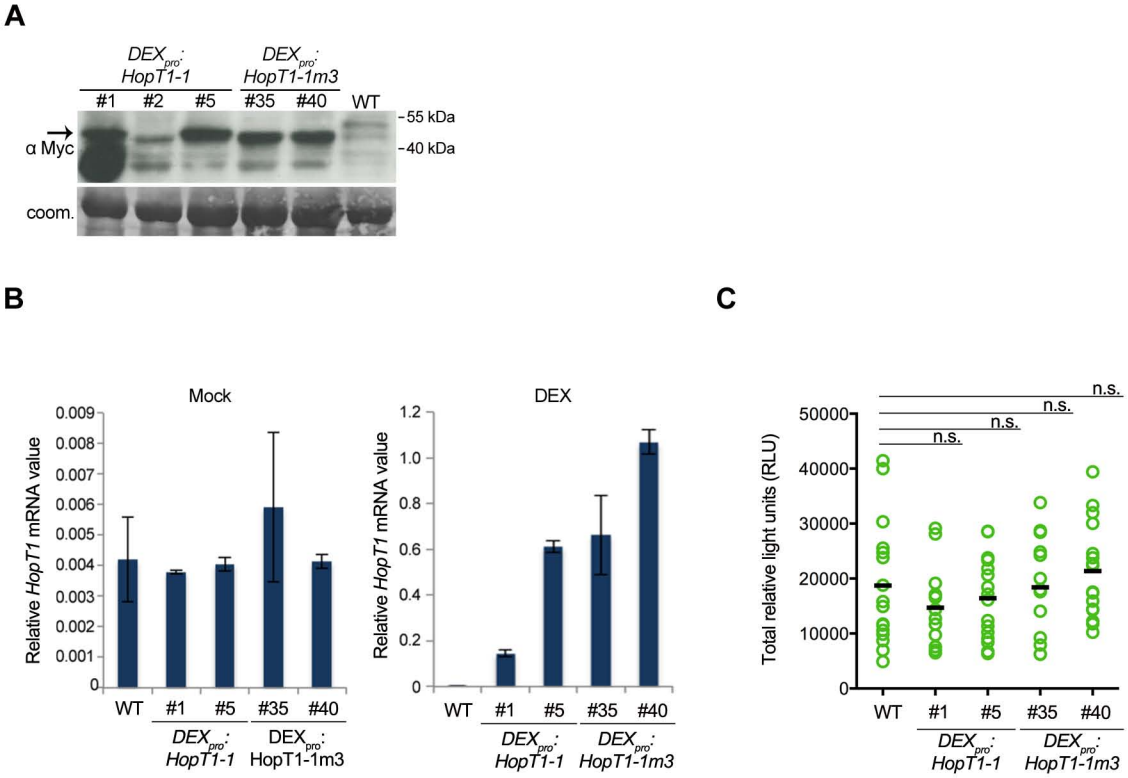

Supplemental Figure 4. Characterization of dexamethasone inducible HopT1-1 and HopT1-1m3 transgenic lines
(A) Five-week-old Arabidopsis Col-0 (WT) plants and T2 transgenic lines expressing Myc-HopT1-1 or Myc-HopT1-1m3 under the control of the dexamethasone inducible promoter (*DEX$_{pro}$:HopT1-1* and *DEX$_{pro}$:HopT1-1m3*, respectively) were sprayed using 30 µM of DEX. After 24 hours, leaves from three plants were collected and pooled together for the transgenic lines as well as for the control line for further analyses. Protein accumulation of HopT1-1 and of HopT1-1m3 was assessed by immunoblotting using anti-Myc antibody. Coomassie staining shows equal protein loading for each sample. Transgenic lines expressing comparable levels of HopT1-1 and of HopT1-1m3 were selected for further analyses. **(B)** The plants described in (A) were sprayed every 24 hours using Mock solution or 30 µM of DEX. Leaves were collected 48 hours post induction. Relative expression quantification of *HopT1-1* and of *HopT1-1m3* transcript level in Mock and DEX-treated plants was done using RT-qPCR analysis. *ACTIN2* was used as a control and the error bars represent the standard deviation from three technical replicates. Mock treated *DEX$_{pro}$:HopT1-1* and *DEX$_{pro}$:HopT1-1m3* lines did not show leaky expression of the respective transcripts. **(C)** ROS production assay upon flg22 treatment was performed on the mock-treated plants described in (B). Each dot represents luminescence (RLU) captured for each technical replicate (n=24) and the mean is indicated by horizontal bar. In mock condition, the HopT1-1 transgenic lines did not exhibit significant reduction in ROS production when compared to WT and HopT1-1m3 plants. Statistical significance was assessed using the ANOVA test (n.s.: p-value>0.05; ****: p-value<0.0001).

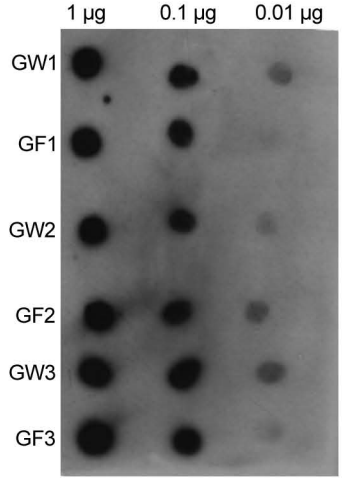

Supplemental Figure 5. Accumulation level of streptavidin-associated peptides containing each GW and GF motifs of HopT1-1 and HopT1-1m3, respectively

To perform the pull-down experiment, we first assessed the accumulation level of streptavidin-associated peptide containing each GW and GF motifs of HopT1-1 and HopT1-1m3, respectively by using dot blot assay. The biotinylated peptides were immobilized with HRP-streptavidin beads and then were spotted on to the nitrocellulose membrane at three different amounts (1 µg, 0.1 µg and 0.01 µg). The presence of peptides was revealed by adding ECL substrate.

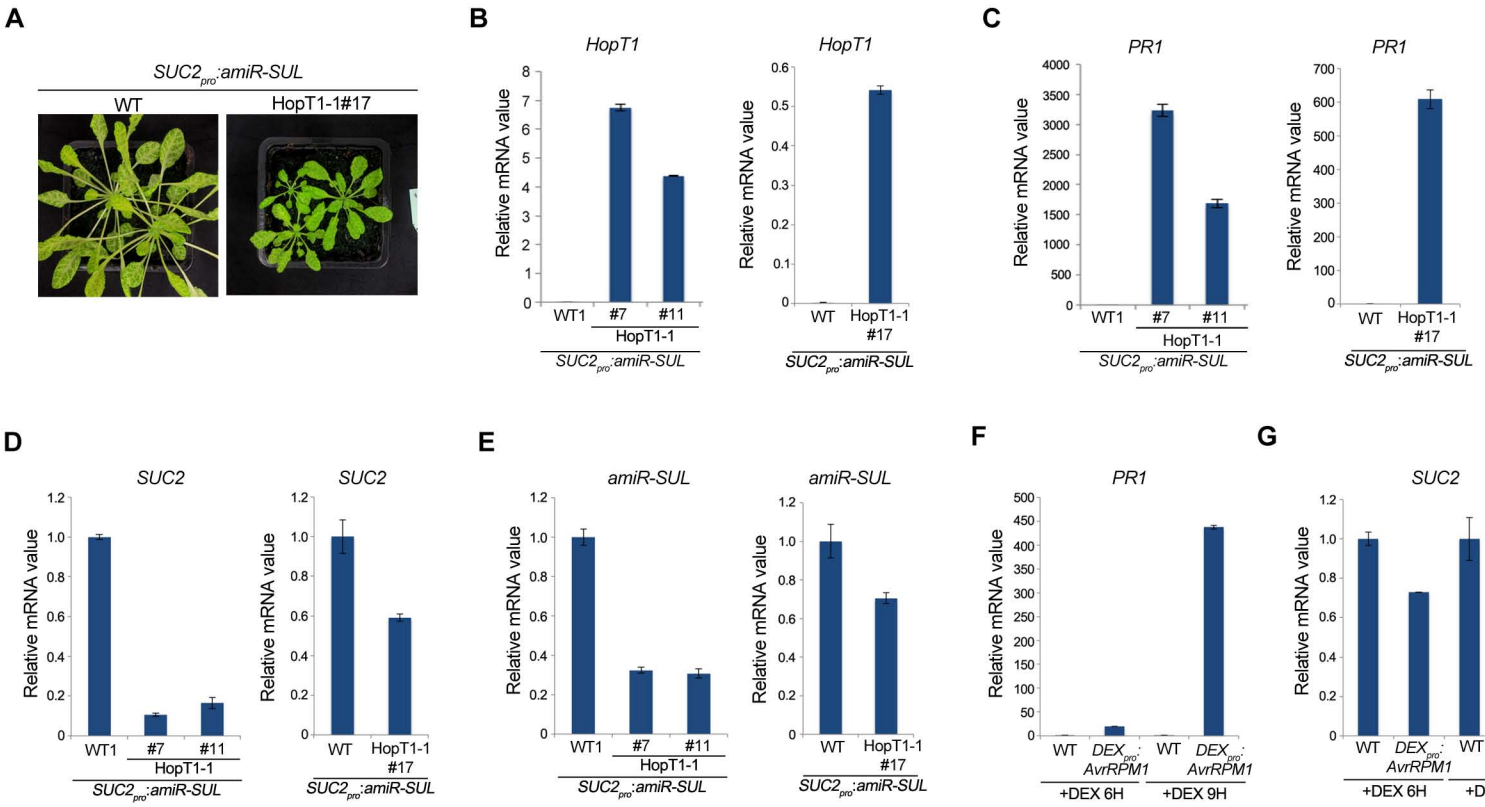

Supplemental Figure 6. ETI response represses the expression of the endogenous *SUC2* gene and of the *SUC2$_{pro}$:amiRSUL* transgene
(A) Representative pictures of five-week-old *SUC2$_{pro}$:amiR-SUL* plants (WT) along with *SUC2$_{pro}$:amiR-SUL* transgenic line overexpressing HopT1-1. The selected HopT1-1#17 transgenic line exhibit intermediate phenotype compared to the lines described in Fig 5.Transgenic lines described in here and in Fig 5 were subjected to further molecular analysis. **(B)** Relative *HopT1* mRNA level was monitored in HopT1-1#17 line by RT-qPCR analysis and the first graph is recapitulated from FigS2 to compare *HopT1* expression level between the different transgenic lines. *Ubiquitin* was used as a control and the error bars represent the standard deviation from three technical replicates. The *HopT1* transcript accumulation in the transgenic line exhibiting intermediate phenotype was approximately 10 times less compared to the lines described in Fig 5. **(C)** Same as in (B), but *PR1* mRNA level was monitored in HopT1-1#17 line and the first graph is recapitulated from Fig5 to compare *PR1* expression level between the different transgenic lines. **(D)** Relative *SUC2* mRNA level was monitored by RT-qPCR analysis using the same samples as described in (B). *Ubiquitin* was used as a control and the error bars represent the standard deviation from three technical replicates. **(E)** Same as in (D) but, relative *amiR-SUL* transgene transcript level was monitored. **(F)-(G)** Five-week-old Col-0 Arabidopsis (WT) plants and *DEX$_{pro}$:AvrRpm1* transgenic plants were sprayed using 30 µM of DEX. Leaves were collected at 6 and 9 hours post treatement to assess the relative mRNA level of *PR1* and *SUC2* transcripts by using RT-qPCR analysis. *Ubiquitin* was used as a control and the error bars represent the standard deviation from three technical replicates.

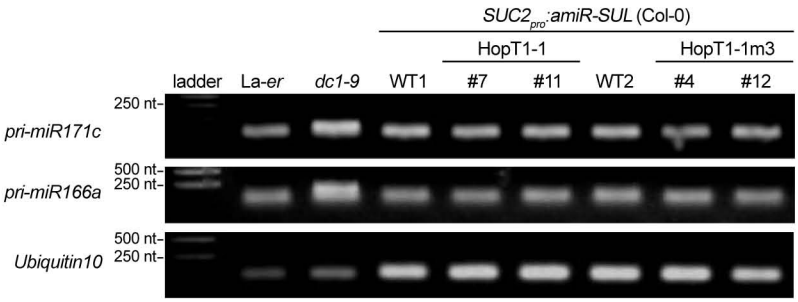

Supplemental Figure 7. The accumulation of the pri-miRNAs, *pri-miR171c* and *pri-miR166a* is not affected in the HopT1-1 transgenic lines
The accumulation level of primary miRNA (pri-miRNA) transcripts of *pri-miR171c* and *pri-miR166a* in the transgenic plants expressing HopT1-1 or HopT1-1m3 compared with WT1 or WT2, respectively was assessed by semi-quantitative RT-PCR analysis. Arabidopsis mutant defective in miRNA biogenesis (*dcl1-9* in La-er background) was used as a control. *Ubiquitin10* was used as a loading control. No significant difference was observed in the accumulation of these pri-miRNAs in the presence of HopT1-1 or HopT1-1m3, respectively.

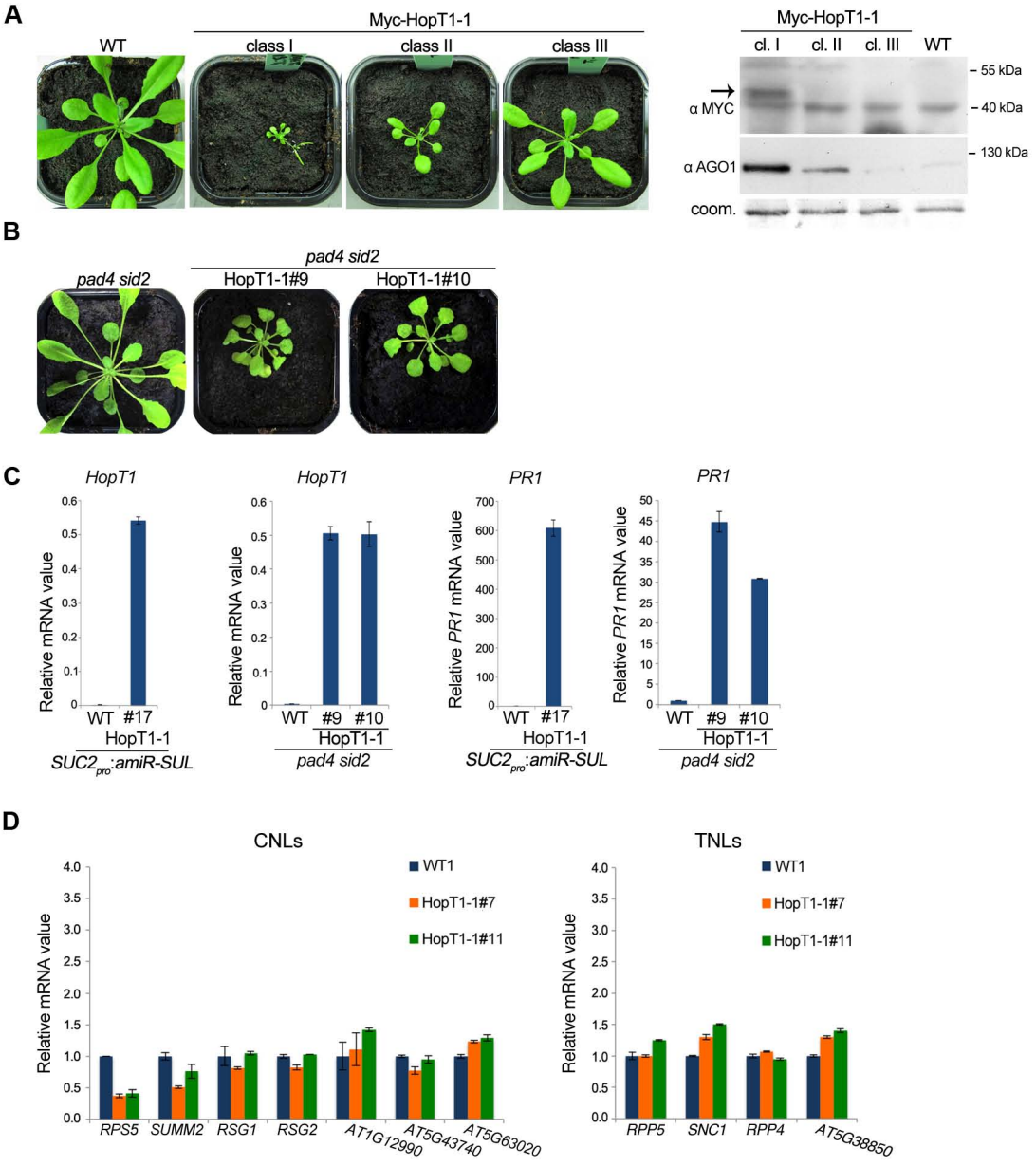

Supplemental Figure 8. Constitutive expression of HopT1-1 *in planta* induces a *PAD4/SID2*-dependent autoimmune phenotype in Arabidopsis
(A) Representative pictures of five-week-old Col-0 (WT) Arabidopsis plants along with three different classes of primary transgenic plants (T1) expressing Myc-HopT1-1. Leaves from plants showing similar phenotype were pooled and used for further molecular analyses. The accumulation level of Myc-HopT1-1 and of AGO1 proteins were assessed by immunoblotting using anti-Myc and anti-AGO1 antibodies. Coomassie staining shows equal protein loading for each sample. Transgenic plants belonging to class I exhibit detectable levels of Myc-HopT1-1 as well as overaccumulation of AGO1 protein when compared to WT plants and other classes, respectively. **(B)** Representative pictures of *pad4-1 sid2-2* plants and transgenic lines expressing HopT1-1 in *pad4-1 sid2-2*. **(C)** Relative mRNA accumulation level of *HopT1* and of *PR1* was performed by RT-qPCR analysis using the same set of data for HopT1-1 expressing *SUC2$_{pro}$:amiR-SUL* transgenic lines as described in FigS6 and the plants expressing HopT1-1 in *pad4-1 sid2-2*. *ACTIN2* was used as control. Error bars represent the standard deviation from three technical replicates. The *pad4-1 sid2-2* double mutations partially compromise the HopT1-1-triggered developmental defects and the SA-dependent defense response. **(D)** Relative mRNA accumulation of CNL or TNL transcripts that are targeted by miRNAs and/or siRNAs was monitored by RT-qPCR analysis in *SUC2$_{pro}$:amiR-SUL* transgenic lines overexpressing HopT1-1. *ACTIN2* was used as control. Error bars represent the standard deviation from three technical replicates. No significant difference was observed in the expression of these genes at the transcript level.

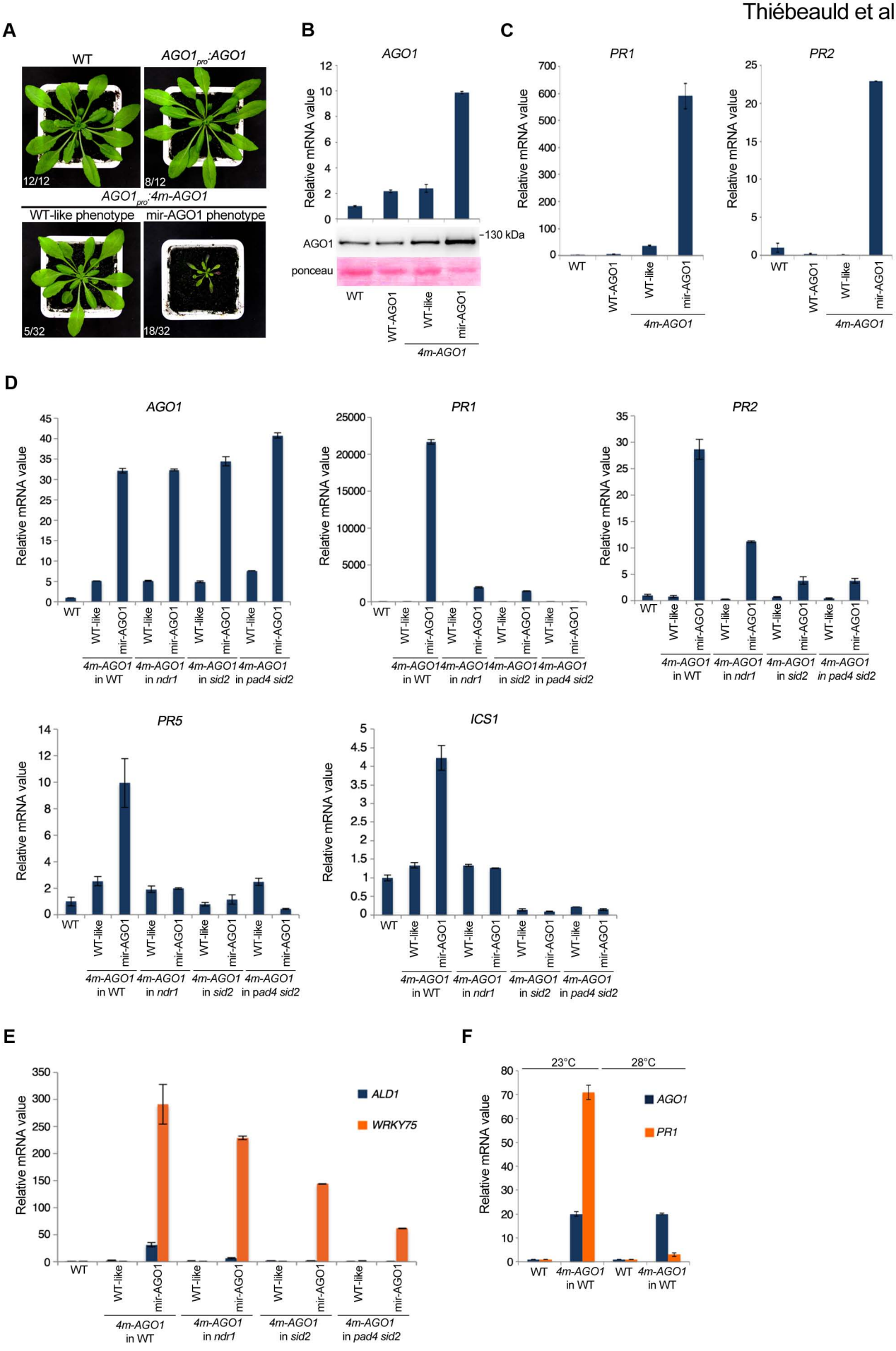
A
WT
AGO1pro:AGO1
12/12
8/12
AGO1pro:4m-AGO1
WT-like phenotype
mir-AGO1 phenotype
5/32
18/32
B
AGO1
Relative mRNA value
AGO1
ponceau
130 kDa
WT
WT-like
mir-AGO1
4m-AGO1
C
PR1
PR2
Relative mRNA value
WT
WT-like
mir-AGO1
4m-AGO1
D
AGO1
PR1
PR2
PR5
ICS1
Relative mRNA value
WT
WT-like
mir-AGO1
4m-AGO1 in WT
4m-AGO1 in ndr1
4m-AGO1 in sid2
4m-AGO1 in pad4 sid2
E
ALD1
WRKY75
Relative mRNA value
F
23°C
28°C
AGO1
PR1
Relative mRNA value
WT
4m-AGO1 in WT

Supplemental Figure 9. Stable expression of an AGO1 transgene that is refractory to miR168 action induces *PAD4/SID2* dependent autoimmune phenotype in Arabidopsis

(A) Representative pictures of six-week-old Col-0 Arabidopsis plants (WT) along with primary transgenic plants (T1) expressing *AGO1*$_{pro}$*:AGO1* (WT-AGO1; upper panel) and miR168 refractory AGO1 transgene *AGO1*$_{pro}$*:4m-AGO1* (*4m-AGO1*; lower panel) under the native AGO1 promoter in WT background. Primary transformants of *4m-AGO1* exhibit two different phenotypes, WT-like and mir-AGO1. mir-AGO1 plants show dwarf and anthocyaned phenotype whereas WT-like plants show normal phenotype similar to WT plants. **(B)** Relative *AGO1* mRNA level in WT plants and in WT-AGO1 as well as in *4m-AGO1* transgenic plants exhibiting WT-like and mir-AGO1 phenotype was monitored by RT-qPCR analysis using *Ubiquitin* as control. Error bars represent the standard deviation from three technical replicates. The accumulation level of AGO1 protein was assessed by immunobloting in the same samples. Ponceau red staining shows equal loading for each sample. **(C)** Relative mRNA accumulation level of SA responsive genes (*PR1* and *PR2*) in same samples as (B) was monitored by RT-qPCR analysis using *Ubiquitin* as control. **(D)** Six-week-old primary transgenic plants (T1 generation) expressing *4m-AGO1* transgene in WT and in different SA signalling mutants (*ndr1-1* and *pad4-1 sid2-2*) and SA biosynthesis mutant (*sid2-2*) exhibiting WT-like and miR-AGO1 phenotypes were collected. Relative mRNA accumulation level of *AGO1* and of SA responsive genes (*PR1*, *PR2* and *PR5*) or gene involved in salicylic acid biosynthesis (*ICS1*) was monitored using RT-qPCR analysis same as described in (B)-(C). **(E)** Relative mRNA accumulation level of cell death and senescence-related markers (*ALD1* and *WRKY75*) in same samples as (D) was monitored by RT-qPCR analysis using *Ubiquitin* as control. **(F)** WT plants and primary transgenic plants expressing *4m-AGO1* transgene were grown in parallel at 23°C and at 28°C. Leaves from four-week-old plants were collected to assess the level of *AGO1* and *PR1* mRNA accumulation by RT-qPCR using *Ubiquitin* as a control.

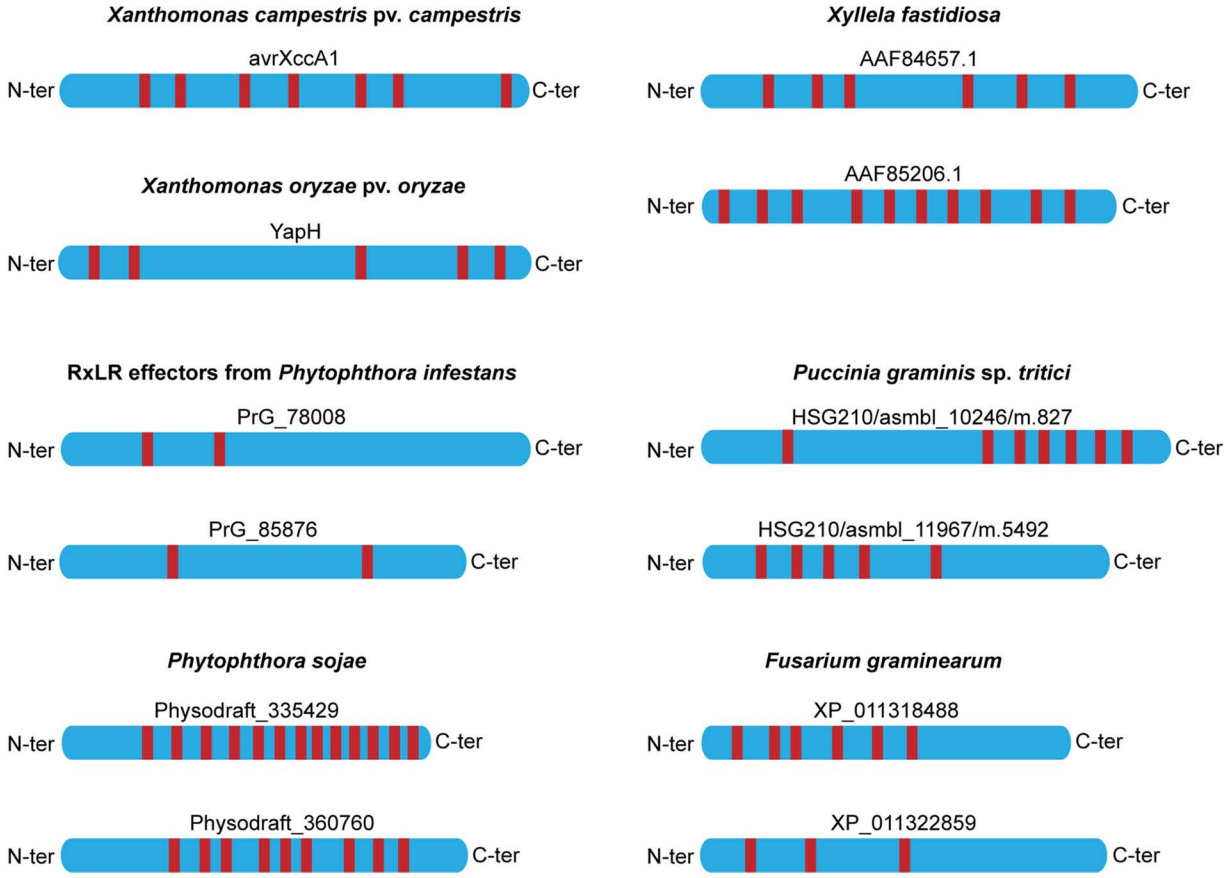

Supplemental Figure 10. Several effectors encoded by agriculturally important phytopathogens contain canonical GW/WG motifs
Effectors encoded by bacteria (*Xanthomonas campestris*, *Xanthomonas oryzae* and *Xyllela fastidiosa*), oomycetes (*Phytophthora infestans* and *Phytophthora sojae*) or fungi (*Puccinia graminis* and *Fusarium graminearum*) containing the highest score (matrix AGO-planVir) of GW/WG motifs prediction were retrieved by using the web portal http://www.comgen.pl/whub (Zielezinski A. & Karlowski WM, 2014). A red bar represents each GW or WG motif.

Table S1, related to Experimental Procedures. Primers used in this study.

Name	Sequence	Remarks
AT5G38850_F	5'-CATGGAACTCAGCTTCACCA-3'	qPCR
AT5G38850_R	5'-GAGACGAACGGTGATGGAAT-3'	qPCR
RPP5_F	5'-TGGGTGCAAGCTCTCACAGA-3'	qPCR
RPP5_R	5'-TCATTAGGCCCGTTCAGAAGA-3'	qPCR
SUMM2_F	5'-AAAACCACCCTTCTCACACG-3'	qPCR
SUMM2_R	5'-TCCCGATGTCTCCTTGAATC-3'	qPCR
AT5G63020_F	5'-TTTCTGTTGTGCAAGGATGG-3'	qPCR
AT5G63020_R	5'-CAACTCTCTCAGCCACCACA-3'	qPCR
AT5G43740_F	5'-CAGCCTGATGAACGATGAAA-3'	qPCR
AT5G43740_R	5'-TGCCCTCGAACTGAAAGTCT-3'	qPCR
AT1G12990_F	5'-CTCTATGGCATGGGTGGAGT-3'	qPCR
AT1G12990_R	5'-TCGACTGCCTTTTGGTTTTC-3'	qPCR
PR1_F	5'- AAAACTTAGCCTGGGGTAGCGG-3'	qPCR
PR1_R	5'-CCACCATTGTTACACCTCACTTTG-3'	qPCR
PR5_F	5'-ATCGGGAGATTGCAAATACG-3'	qPCR
PR5_R	5'-GCGTAGCTATAGGCGTCAGG-3'	qPCR
PAD4_F	5'-GGCGGTATCGATGATTCAGT-3'	qPCR
PAD4_R	5'-CGGTTATCACCACCAGCTTT-3'	qPCR
ICS1_F	5'-TGGTTAGCGTTGCTGGTATC-3'	qPCR
ICS1_R	5'-CATTCAACAGCGATCTTGCC-3'	qPCR
HAP2B_F	5'-TGCTGCAATTTCAAAACCTG-3'	qPCR
HAP2B_R	5'-GCCAAAGATGATTTGCCTGT-3'	qPCR
AGO1_F	5'-AAGGAGGTCGAGGAGGGTATGG-3'	qPCR
AGO1_R	5'-CAAATTGCTGAGCCAGAACAGTAGG-3'	qPCR
AGO2_F	5'-GCCCCAATAACGCAGTTTTA-3'	qPCR
AGO2_R	5'-CAAATTCGTTTCAACACACCA-3'	qPCR
MYB33_F	5'-GACATTCACCTGTTATGATT-3'	qPCR
MYB33_R	5'-TGGAGACTGAATGTAAGTAT-3'	qPCR
CKB3_F	5'-ATGTACAAGGAACGTAGTGG-3'	qPCR
CKB3_R	5'-CTAGATGTGGTGGTGGAAGT-3'	qPCR
DCL1_F	5'-GCACCGTTTGAAATACTTGAGG-3'	qPCR
DCL1_R	5'-CGCTACTCCAACTTGAACACC-3'	qPCR
CCS_F	5'-CCCATATGACAGTACCATCA-3'	qPCR
CCS_R	5'-CCATTTCAAGATCAAACTGGCAC-3'	qPCR
PR2_F	5'- GCTTCCTTCTTCAACCACACAGC-3'	qPCR
PR2_R	5'-CGTTGATGTACCGGAATCTGAC-3'	qPCR
SUC2_F	5'-GACCCATGTGGATGCTTCTT -3'	qPCR
SUC2_R	5'-AGCTCTGACTCCGTCGTTGT-3'	qPCR
SUL_F	5'-GCTTAGGCCACAGCTTCTTG-3'	qPCR
SUL_R	5'-AGGTTTGCCCTAGCAGTTGA-3'	qPCR
amiR-SUL_F	5'-CGAATTGGGTACCGGGC-3'	qPCR
amiR-SUL_R	5'-CTAGAACTAGTGGATCCCCC-3'	qPCR
HopT1-1_qPCR_F	5'-GGCTAGCGAAAGTCGTGAAC-3'	qPCR
HopT1-1_qPCR_R	5'-AACCCTTATCGAAGCCCACT-3'	qPCR
UBQ10_F	5'-GGCCTTGTATAATCCCTGATGAATAAG-3'	qPCR
UBQ10_R	5'-AAAGAGATAACAGGAACGGAAACATAGT-3'	qPCR
miR166a_F	5'-CTGGCTCGAGGACTCTGG-3'	Sq-PCR
miR166a_R	5'-TGGAGTAAACAGGGAGCAACA-3'	Sq-PCR
miR171c_F	5'-ATGTGGATGGAGTTTGGTGTAA-3'	Sq-PCR
miR171c_R	5'-GTGATATTGGCACGGCTCA-3'	Sq-PCR

amiRSUL_RT	5'-GTCGTATCCAGTGCAGGGTCCGAGGTATTCGCACTGGATACGACAGGGAT-3'	RT
miR156_RT	5'-GTCGTATCCAGTGCAGGGTCCGAGGTATTCGCACTGGATACGACGTGCTC-3'	RT
miR160_RT	5'-GTCGTATCCAGTGCAGGGTCCGAGGTATTCGCACTGGATACGACTGGCAT-3'	RT
miR168_RT	5'-GTCGTATCCAGTGCAGGGTCCGAGGTATTCGCACTGGATACGACTTCCCG-3'	RT
amiRSUL_F	5'-GGCGGCTTAAGTGTCACGGAA-3'	qPCR
miR156_F	5'-GCGGCGGTGACAGAAGAGAGT-3'	qPCR
miR160_F	5'-GGCGTGCCTGGCTCCCTGT-3'	qPCR
miR168_F	5'-CGCGTCGCTTGGTGCAGGT-3'	qPCR
Universal_R	5'-GTGCAGGGTCCGAGGT-3'	qPCR
P4835	5'-CACCACCCTCTTACGGACAAGA-3'	deletion of *hopT1-1*
P4836	5'-GGGTATCGAGTGATTGCTGA-3'	deletion of *hopT1-1*
P4837	5'-CACCTCTCAAGGAAAGGCTTGAT-3'	deletion of *hopT1-1*
P4838	5'-GAAACGTTTGTCTCCGGCTA-3'	deletion of *hopT1-1*
P4839	5'-CACTTGAACGAGATCGCAGA-3'	deletion of *hopT1-1*
P4840	5'-GCATCAAGCCTTTCCTTGAG-3'	deletion of *hopT1-1*